Journal of Power Sources 195 (2010) 2036–2043

Contents lists available at ScienceDirect

Journal of Power Sources

journal homepage: www.elsevier.com/locate/jpowsour

Decomposition of ethylene carbonate on electrodeposited metal thin film anode

Jean-Sebastien Bridel[a], Sylvie Grugeon[a], Stephane Laruelle[a], Jusef Hassoun[b], Priscilla Reale[b], Bruno Scrosati[b], Jean-Marie Tarascon[a,*]

[a] Laboratoire de Reactivité et Chimie des Solides, Université de Picardie Jules Verne CNRS (UMR-6007), Faculté des Sciences, 33 rue Saint-Leu 80039, Amiens Cedex, France
[b] Chemistry Department, University of Rome "La Sapienza", 00185 Roma, Italy

ARTICLE INFO

Article history:
Received 4 September 2009
Received in revised form 13 October 2009
Accepted 14 October 2009
Available online 23 October 2009

Keywords:
Li-ion batteries
Electrolytes
Li alloys
Negative electrodes

ABSTRACT

Metals capable of forming alloys with Li are of great interest as an alternative to present carbon electrodes, hence the importance of knowing their interactions with electrolytes is necessary. Herein we report further on the high-voltage extra irreversibility of Sn electrodeposited thin films vs. Li in EC–DMC 1 M $LiPF_6$ electrolytes. We show that this high-voltage irreversibility is strongly dependent upon the electrolyte composition as demonstrated by its disappearance in EC-free electrolytes. This finding coupled with IR spectroscopy measurements provides direct evidence for the tin-driven catalytic degradation of EC during the discharge of Sn/Li cells. From an electrochemical survey of various metals, capable of alloying with Li, we found that Bi and Pb behaved like Sn while Si and Sb did not act as catalysts towards EC degradation. A rationale for such behaviour is proposed, a procedure to bypass EC degradation with the addition of VC is presented, and an explanation for the non-observance of catalytic-driven EC degradation for Sn/C composites is provided.

1. Introduction

Li-ion technology has conquered the portable battery market and stands as a serious contender for EV and HEV applications. However, for large volume applications, besides the need for higher energy density and power rate electrodes, safety and cost issues must be overcome. In order to address this challenge, a wide variety of research directions enlisting different Li reactivity mechanisms (conversion, displacement and alloying reactions) as compared to the classical Li insertion mechanism have been explored with varying levels of success.

The ability to electrochemically obtain well-defined intermetallic lithium alloys can be traced back to the 1970s owing to the awareness that some of them (Li–Al [1], Li–Si [2], Li–Sb [3], Li–Bi [4]) could lead to staggering specific and volumetric capacity gains as compared to graphite electrodes. For example, the electrochemical reaction of tin with Li leads to several room temperature alloys, LiSn, Li_5Sn_2, $Li_{13}Sn_5$, Li_7Sn_2 and $Li_{22}Sn_{15}$, as reported earlier on by Huggins [5] and later confirmed by Courtney and Dahn via *in situ* X-ray diffraction [6], with the latter corresponding to a theoretical capacity of 994 mAh g^{-1} as compared to 372 mAh g^{-1} for today's carbon electrode.

An inherent drawback to electrodes based on alloys results from their poor cycling life (e.g., rapid capacity fading) [7] caused by large volume swings upon subsequent charges/discharges, which results in an electrochemical grinding of the electrode, and therefore its electric percolation loss [7]. The first suggested solution was to use electrodes made of nanoparticles as the usual mechanisms of deformation and dislocation are not the same as the micro-scale [8], because the smaller particles are capable of releasing strains without fracturing. Other approaches to maintain electrode integrity enlist either (1) the preparation of metal thin films, which provide the best electrical contact via their strong adherence to the substrate [9], hence preserving high quality electrical contact during cycling, or (2) the fabrication of (metal–carbon-binder) composite electrodes with an appropriate binder so that Si/C/carboxy-methyl-cellulose (CMC) electrodes with attractive cycling properties were achieved [10,11] or (3) the elaboration via the pyrolysis of organic precursors of metal–carbon (Si/C, Sn/C) composites [12] with the carbon acting as a volume buffer matrix. Regarding the latter approach, Sn/C nanostructured composites prepared by infiltration of an organo-metallic tin precursor into an organic resorcinol–formaldehyde gel followed by calcinations under argon [13], were shown to display outstanding cycling performances with 50% irreversible capacity between the first discharge and charge cycle. Unless we remove this irreversible capacity, the use of such electrodes in practical Li-ion cells will remain an unlikely scenario.

Understanding these large irreversible capacities has been the subject of numerous studies. It is commonly agreed that they cannot be explained by the classic solid electrolyte interface formation (SEI); however there are divergences on other possible causes such

* Corresponding author. Tel.: +33 03 22 82 75 72; fax: +33 03 22 82 15 90.
E-mail address: jean-marie.tarascon@u-picardie.fr (J.-M. Tarascon).

0378-7753/$ – see front matter © 2009 Elsevier B.V. All rights reserved.
doi:10.1016/j.jpowsour.2009.10.038

as the irreversible decomposition of amorphous surface oxide layers, the presence of remaining impurities within the carbon matrix and the large catalytic activity of Sn nanoparticles towards electrolyte decomposition. Interestingly, large irreversible capacities were independently reported [14–16] for an electrodeposited tin electrode with the appearance of a high-voltage irreversible capacity phenomenon at around 1.5 V during the first lithiation. Beaulieu et al. [17] showed by *in situ* AFM that this extra capacity was associated with the formation of a thick decomposition product layer. This layer, which inhibited the Li-ion diffusion, was put forward as the source of the poor recharge of the electrodeposited tin thin film electrode. In 2003, Beattie et al. [15] showed that the irreversible capacity and the discharge rate were correlated, and he speculated that pure Sn has a crystal face that acts as a catalyst for electrolyte decomposition. The authors succeeded in eliminating the 1.5 V phenomena by either alloying Sn with Cu or short-circuiting the cell (e.g., forcing Sn lithiation), both of which prevent the presence of a pure Sn/electrolyte interface.

So in light of these considerations, one wonders if there is a common link between the large irreversible capacity observed in both Sn/C composites and electrodeposited thin films. In order to answer such a question we embarked on a full study of the effect of various electrolyte compositions, cycling conditions, and other electrochemically active metals towards Li besides Sn, such as Bi and Pb, on the amplitude of the 1.5 V phenomena. The paper reports a systematic approach, which reveals that adding EC to the electrolyte can trigger the appearance of the 1.5 V phenomena, hence enabling the formulation of suitable electrolytes to properly cycle Sn electrode and limit the irreversible capacity. For reasons of clarity, the paper will be structured as follows. The growth of the electrochemical deposits is described first, followed by a description of the morphological changes of the film during lithiation (as deduced by Scanning Electron Microscopy (SEM)) together with the nature/composition of the decomposition layer (as deduced by IR). Then this methodology is extended to various electrolytes and different metal elements alloying with Li. Finally a tentative explanation will be given to explain the specificity of Sn in producing such electrolyte decomposition and our failure to eliminate the irreversible capacity in Sn/C composites.

2. Experimental

All the metallic thin films made during the course of this study were electroplated on stainless steel disks (AISI 304, Goodfellow), which were polished to a mirror finish, and then successively rinsed with water, ethanol and acetone before drying. These disks, positioned horizontally, were used as working electrodes in a one-compartment three-electrode cell in which the temperature was set and maintained at 25 °C via a water-circulating thermostat. Platinum and a saturated mercury-mercurous sulphate electrode (MSE) (E_{eq} = 0.64 V/ENH) were used as anode and reference electrode, respectively. The electrolytic baths were constantly purged with nitrogen gas to both reduce the oxygen concentration and prevent the oxidation of the precursors; their composition depended on the type of metal to be deposited.

For tin electrodeposit, the bath was composed of a mixture of H_2SO_4 (0.6 M) and $SnSO_4$ (0.3 M) solution to which we added a surfactant agent (2×10^{-3} M) N,N-bi deca oxyethylene octadecylamine, commercially called Amiet THD/32 Kao Corp [18]. The films were deposited at a potential of −1.25 V/SEM with a Coulomb limitation of −3 C.

The electrodeposited bath for lead was a solution mixture of $PbSO_4$ (0.05 M) and NaOH (0.4 M) and the deposition potential was −1.6 V/MSE with a Coulomb limitation of −1.72 C.

For bismuth, the bath was composed of a mixture of $Bi(CH_3COO)_3$ (0.01 M) and "Pyrocatechol violet" ($C_{19}H_{14}O_7S$, 0.02 M) in aqueous acid medium [19], and the films were deposited at a potential of −0.53 V/SEM with a Coulomb limitation of −1.7 C.

Antimony thick films were deposited from a solution mixture containing Sb_2O_3 (0.08 M) and citric acid (0.2 M) at a potential of −1.15 V/MSE with a Coulomb limitation of −4.4 C [20].

Last, silicon deposits were made according to Nishimura's recipe [21] in inert atmosphere, in a potentiostatic mode at −3.6 V vs. Pt, from a propylene carbonate electrolytic bath containing 0.5 M of tetrachlorosilane ($SiCl_4$) and 0.1 M of tetrabutylammonium chloride.

Regardless of the deposited metal elements, all the films were washed with distilled water or propylene carbonate in case of silicon and dried prior to being structurally and electrochemically characterized. Undoubtfully, this washing treatment done under air, leads to the creation of an oxide film at the surface of our films.

Electrochemical tests of these films, whose weight was ranging from 1 to 2 mg as estimated from the electrodeposit currents assuming 100% Coulomb efficiency, were performed using coin cells (standard 2035-size) that were assembled in an argon filled dry-box. The electrodeposited thin metal sample was separated from a lithium disk that was used as the negative electrode by a borosilicate micro-fibre (Millipore) film impregnated, if not otherwise specified, with 0.5 mL of 1 M $LiPF_6$ in ethylene carbonate (EC), dimethyl carbonate (DMC) (1:1 in weight) electrolyte solution. Other tested solvents: EC, DMC and THF (grade "selectipur"), purchased from Merck and lithium hexafluorophosphate from Sigma–Aldrich, were used as received without any extra purification or drying steps. The electrochemical data were collected using an automatic multi-potentiostat system (VMP – Biologic SA, Claix, France) operating in galvanostatic mode at 20 °C in the 0.01–2 V potential window. The potential values are given vs. Li^+/Li and the current densities are expressed in milli-ampere per cm^2 of electrode surface, as the current density by active surface is difficult to estimate in thin films.

After being cycled, the cells were carefully opened in an argon filled dry-box. Electrodes were rinsed with acetonitrile in order to eliminate residual traces of solvents and salts. Scanning electron microscopy studies were performed by means of a FEI® Quanta 200 FEG (by using airlock chamber) coupled with an Oxford X-ray micro-analyzer (Link Isis). Infrared spectra were recorded on a Nicolet Fourier transform AVATAR 370 DTGS infrared spectrometer working in the 4000–400 cm^{-1} spectra range equipped with attenuated total reflectance (ATR) and a Ge crystal working in the 4000–700 cm^{-1} spectra range (resolution: 4 cm^{-1}). Measurements are performed, under argon atmosphere, directly from the cycled electrodeposited disc after washing.

3. Results

3.1. High-voltage extra capacity in tin thin film

The charge–discharge curve for an electrodeposited thin film discharged cycled in presence of 1 M $LiPF_6$ in EC/DMC electrolyte at a current density of 40 μA cm^{-2} (20 mA g^{-1}) is shown in Fig. 1. The voltage initially drops, attains a sharp minimum prior to reaching a long plateau located near 1.5 V, and then abruptly deviates from 1.5 V to reach a lower voltage plateau near 0.45 V; the latter corresponds to the range of potentials at which Li alloys with Sn form various Li_xSn phases. We experienced that the amplitude of the 1.5 V plateau is extremely sensitive to the reduction current so that no high-voltage plateau is observed at high current density (more than 0.05 mA cm^{-2}). In contrast, by lowering the current density to 10 mA g^{-1} (20 μA cm^{-2}) we reach a plateau capacity as high as 1422 mAh g^{-1} (4.5 mAh cm^{-2}). Additionally, we observed a one to one direct relationship between the plateau amplitude capacity

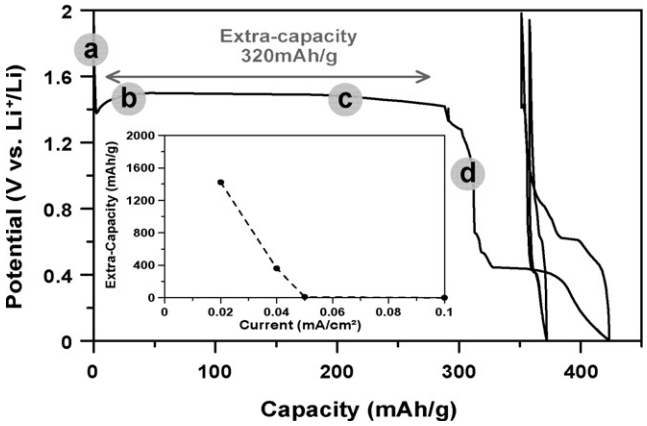

Fig. 1. Sn/Li cell voltage vs. capacity at 40 μA cm^{-2} (20 mA g^{-1}) in EC–DMC 1 M $LiPF_6$ showing the high-voltage extra capacity at 1.5 V together with an inset of the 1.5 V plateau capacity dependence with applied specific current. The added a–d letters symbolize the cut-off voltage for each sample studied by SEM.

and the cell cycling capability; with the largest (1.5 V) plateau cell showing the poorer cyclability (e.g., capacity retention).

SEM was used to check the tin thin film morphology upon cycling. For this study several coin cells using an electrodeposited tin film as positive electrode were discharged at a current of 40 μA cm^{-2} (20 mA g^{-1}), and stopped at different states of discharge indicated by labelled circles in Fig. 1. The as-made film (Fig. 2a) displays a homogeneous and granular surface. As the Li electrochemical reduction proceeds (Fig. 2b), small particles appear on the surface of the film together with the growth of a thin extra-layer. Further reduction (Fig. 2c) results in a coarsening of this layer to form islands, which finally cover (Fig. 2d) the entire surface of the tin electrodeposited film. By tilting the sample we were able to estimate the thickness of the deposit film which averages 2–3 μm. In parallel, complementary energy dispersive spectroscopy analyses have been performed on the as-made (a) and partially lithiated (b, c and d) films; we note that the growth of the concomitant island shows increased carbon and oxygen signals as compared to the tin signal, which could be indicative of the formation of a C–O rich inorganic phase (e.g., Li_2CO_3) or organic deposits during the reduction process or both as it will be demonstrated hereafter by IR spectroscopy. Such electrochemically driven changes in morphology did not come as a surprise as they were similar to what has been reported by Dahn [17].

Infrared spectroscopy was used to grasp further insight into the chemical nature of the "organic" deposit which forms upon the electrochemical reduction of the tin electrodeposited films. Fig. 3 shows a comparison between the IR spectrum of the film recovered from a Sn/Li coin cell, which was discharged until the end of the 1.5 V plateau (e.g., referred to as d in Fig. 1), and those of pure Li_2CO_3 and CH_3OCO_2Li. The IR spectrum for the reduced sample shows a

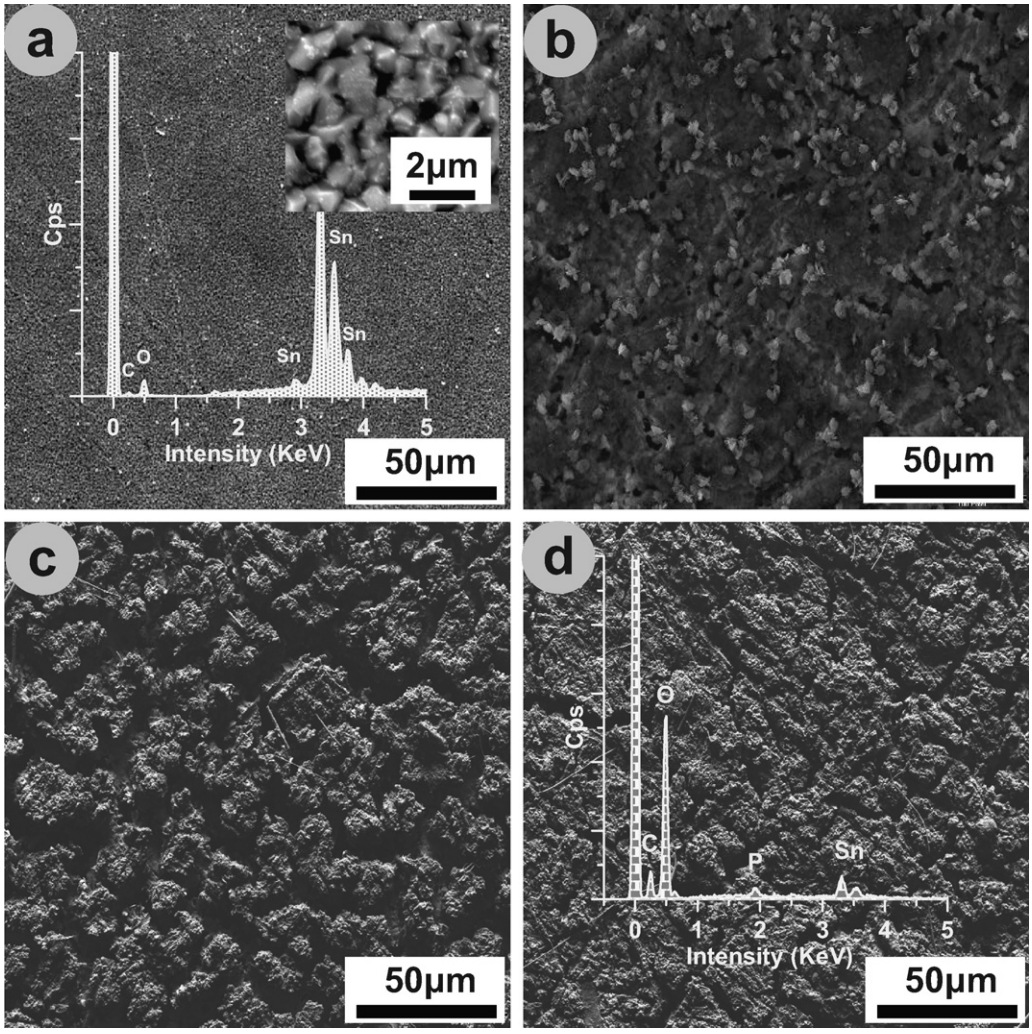

Fig. 2. Scanning electron microscopy image of tin film stopped at different states of discharge indicated by labelled circles in Fig. 1 together with EDS spectra.

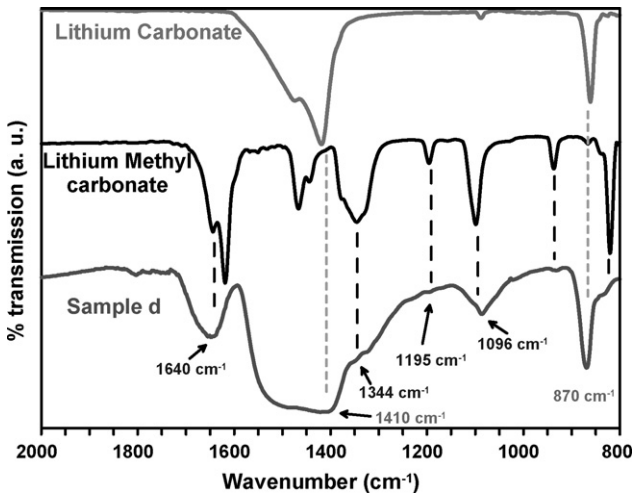

Fig. 3. Infrared spectrum (ATR) of lithium carbonate, lithium methyl carbonate and Sn surface of a Sn/Li cell stopped at a 1 V cut-off voltage (labelled d in Fig. 1).

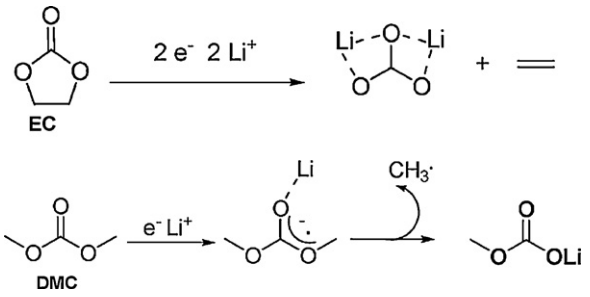

Scheme 1. Reaction decomposition of EC and DMC.

band located at 870 cm^{-1} and another broad one between 1550 and 1400 cm^{-1}, which corresponds to the IR signature of Li_2CO_3, thus indicating a copious amount of lithium carbonate at the film surface. Although quite less pronounced, the IR spectrum of the reduced sample shows extra bands which simply correspond (dark dashed lines in Fig. 3) to the presence of lithium methyl carbonate CH_3OCO_2Li. The formation of these two compounds involves the reduction of EC and DMC [22–24] according to the reaction (Scheme 1).

Assuming then that the 1.5 V plateau corresponds only to the reduction of EC, and knowing the theoretical density of lithium carbonate and the numbers of Coulomb released during this anomalous plateau, we were able to estimate a thickness value (~1 μm) for the deposit which is consistent with the value observed by microscopy.

To confirm the direct link between the 1.5 V plateau and the EC degradation, Li/Sn coin cells using free-EC electrolytes and more specifically DMC 1 M $LiPF_6$, PC 1 M $LiPF_6$ and THF 1 M $LiPF_6$ electrolytes were assembled and discharged under the same conditions as before (e.g., using the same current rate). A distinct feature of the collected discharge curves (Fig. 4) is the absence of the 1.5 V plateau which confirms our hypothesized link between EC and this plateau; this was also supported by SEM studies which did not reveal the existence of decomposition products islands at the surface of electrochemically reduced tin electrodeposits. It is worth noting that in the case of PC–1 M $LiPF_6$, there is the appearance of a small plateau at around 2.25 V, which slightly varies with varying the current density. The benefits of using EC-free electrolytes are twofold. As the material surface is no longer poisoned by a thick layer of decomposition products, the electrodes can deliver much larger capacities during the first reduction, 500–600 mAh g^{-1}, at 0.45 V as compared to only 100 mAh g^{-1} for cells using EC–DMC 1 M $LiPF_6$ mixtures.

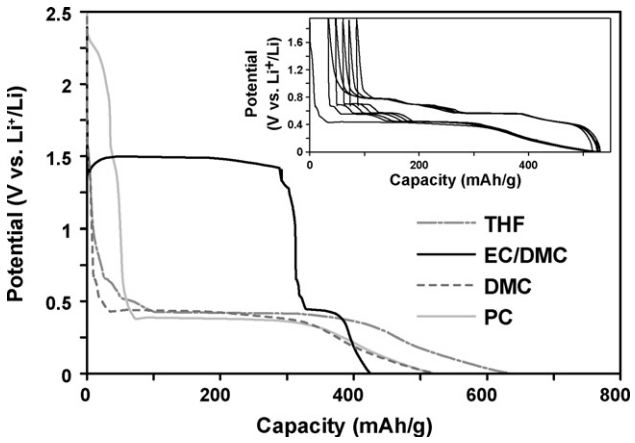

Fig. 4. First discharge voltage–capacity traces for a Sn/Li cell in THF, EC/DMC, DMC and PC with 1 M $LiPF_6$ at 40 μA cm^{-2} (except for the PC: 5 μA cm^{-2}) together with an inset of the DMC–1 M $LiPF_6$ electrolyte four next cycles showing the reversibility.

Additionally, owing to the lower interfacial resistance, the capacity retention of Li/Sn cells cycled in EC-free electrolytes is drastically improved (Fig. 4 inset).

A straightforward solution to bypass the encountered problems in cycling Sn electrodes will be to deviate from EC-based electrolytes. However, this is not a viable option because most of today's Li-ion batteries rely on the use of such electrolytes. Fortunately, alternatives to control electrolyte decomposition/SEI formation do exist with the most successful one enlisting the use of additives termed as "SEI precursors" such as vinylene carbonate (VC) presently used in most of today's commercial Li-ion cells. VC is known to improve the cyclability of some electrodes [25,26] because it can be reduced prior to other electrolyte solvents [27] leading to the formation of an organic-rich SEI layer which provides a better surface passivation than films made of Li inorganic salts. On that basis, two Li/Sn cells were assembled using an EC–DMC 1 M $LiPF_6$ electrolyte solution to which we added 2% and 10% VC, respectively. The benefits are straightforward as we observed (Fig. 5) a 33% and 100% decrease in the 1.5 V plateau, respectively.

IR spectra (Fig. 6) were collected for various tin films recovered from the full discharge of Li/Sn cells using (a) $LiPF_6$/EC + DMC, (b) $LiPF_6$/EC + DMC + 2%wt VC, and (c) $LiPF_6$/EC + DMC + 10%wt VC and compared with the spectrum of pure synthesized poly-VC (Fig. 6d). The IR spectrum for the 2% VC sample is relatively similar to the VC-free one. It reveals the presence of Li_2CO_3 and Li alkyl carbon-

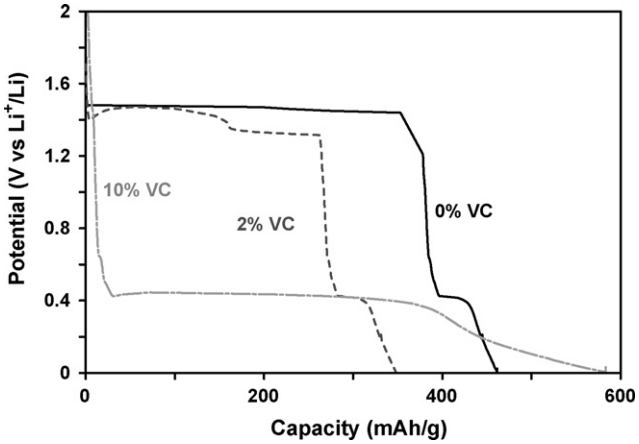

Fig. 5. Galvanostatic first discharge profile (40 μA cm^{-2} or 20 mA g^{-1}) of Sn/Li cells with free-VC, 2 and 10% of VC amount in EC/DMC 1 M $LiPF_6$ electrolyte.

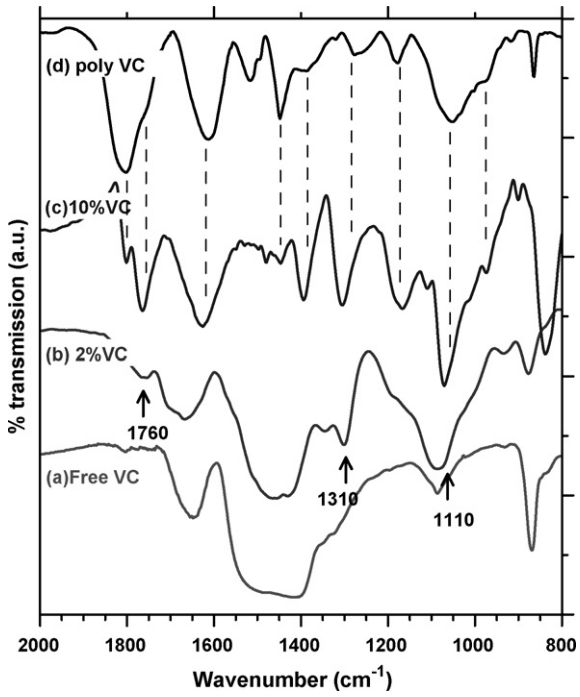

Fig. 6. Infrared spectrum (ATR) of a Sn electrode after the first reduction ($40\,\mu A\,cm^{-2}$) in EC/DMC 1 M $LiPF_6$ with (a) 0%, (b) 2%, (c) 10% of VC and (d) synthesized poly-VC.

ate, as well as weak absorption bands, namely at 1760, 1310 and 1110 cm^{-1} (arrows in Fig. 6b), which suggest the presence of other degradation products, most likely due to the presence of VC. The film cycled with 10% VC-containing electrolyte presents a notably different IR spectrum with the disappearance of, among others, the Li_2CO_3 bands. Additionally there is an increase in the intensity of the bands at 1760, 1310 and 1110 cm^{-1} and the onset of new bands at 1630, 1400 and 840 cm^{-1} suggesting the presence of poly-VC, as deduced by simple comparison to our poly-VC reference sample (Fig. 6d). We note a shift in some bands position, but we believe that it may be due to polymerization degree/organization differences between the chemically and electrochemically synthesized poly-VC. These different IR spectra show that 2% of VC in the electrolyte is not sufficient to prevent the Li_2CO_3 formation from the surface covering. This could imply some competition between the degradation potentials of EC and VC in the considered electrolytes.

3.2. Other metallic elements

At this juncture the question remains whether this anomalous high-voltage irreversible capacity is specific to Sn or does exist with other metallic elements capable of forming alloys with Li. Our group recently reported that a similar phenomenon does occur with Bi electrodeposited thin film which presents a 1.6 V irreversible plateau [19] when electrochemically discharged vs. Li. In order to test whether this phenomenon is universal, we have made various electrodeposited films of bismuth, lead, antimony, silicon, checked their morphologies and tested their electrochemical reactivity vs. Li in the presence of EC-based electrolytes. The SEM pictures for the different films, reported in Fig. 7, indicate quite different morphologies/textures depending upon the nature of the deposited metal? The lead and tin electrodeposited films are somewhat alike and made of one micrometer-sized particles, while the Bi film consists of needle-like particles having dimensions in the 100 nm range. On the contrary, both Sb and Si films are quite dense and do not show a highly granular surface.

The aforementioned metal electrodeposited films were electrochemically tested vs. Li with EC-based electrolytes using the same discharge protocol (Fig. 8a). For all samples we measured the extra capacity at high voltages (e.g., near 1.4–1.6 V) and reported it as a function of the current rate (Fig. 8b). From these results, depending on their reactivity, the metal elements can be parted in two groups. One group, enlisting Si and Sb represented by horizontal lines in Fig. 8b, and for which there is no extra capacity at high

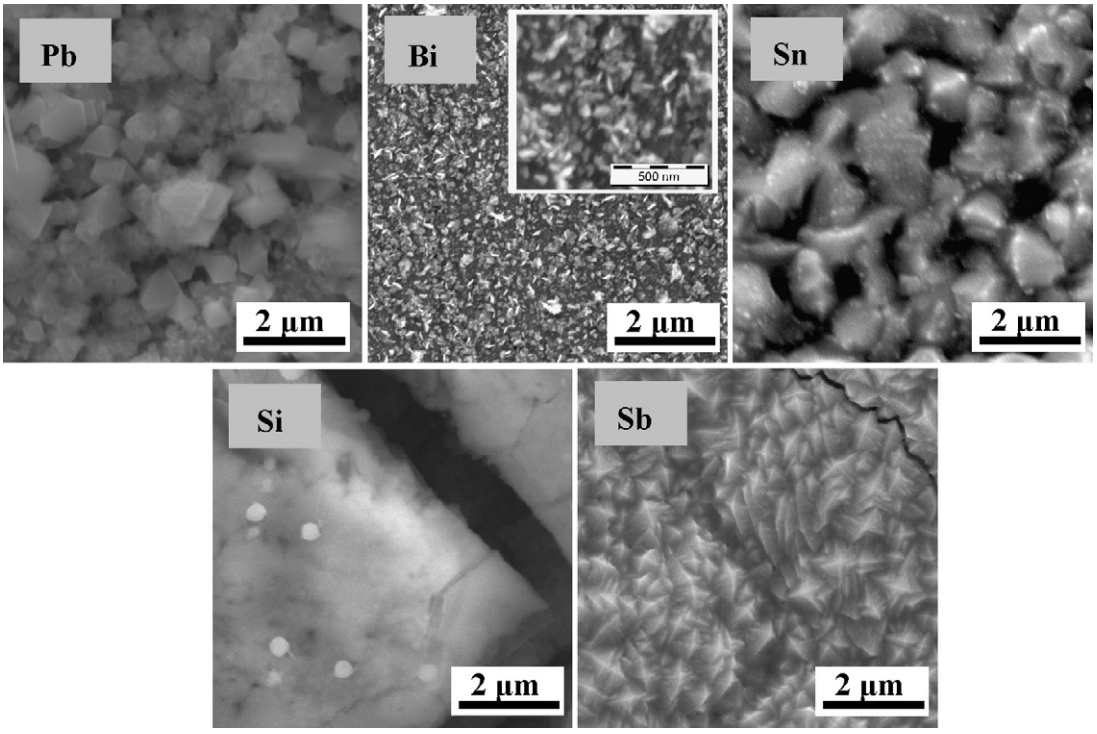

Fig. 7. Scanning electron microscopy images of Pb, Bi, Sn, Si, and Sb electrodeposited film surface.

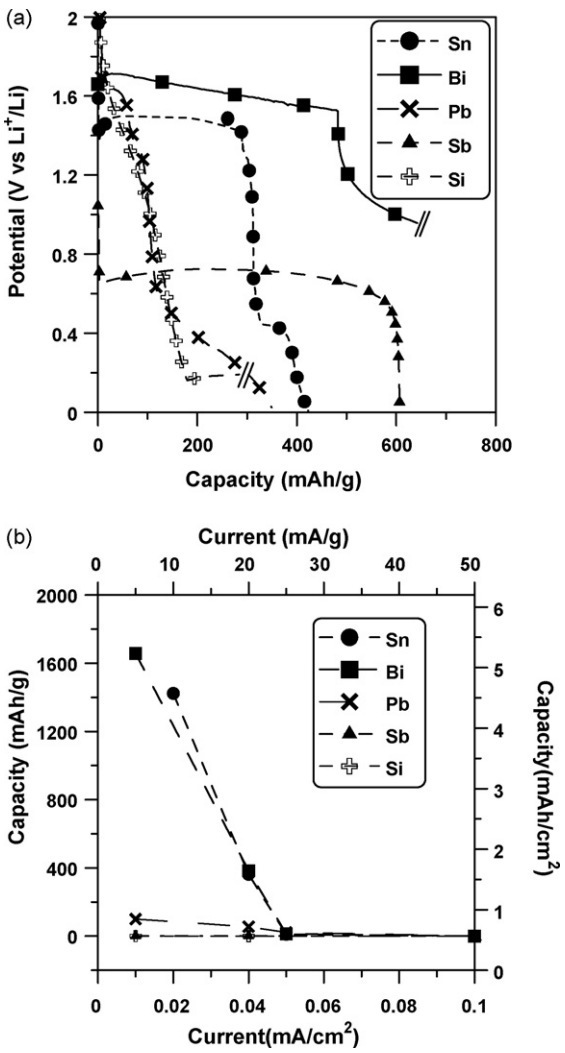

Fig. 8. (a) First discharge voltage–capacity traces for Sn, Pb, Sb, Bi and Si cell in EC–DMC 1 M $LiPF_6$ (40 μA cm^{-2}). (b) "1.5 V plateau" capacity vs. applied current rate curve for the different electrodeposited thin films.

voltage (Fig. 8a), hence zero capacity dependence with current. The remaining Sn, Bi, and Pb can be reunited in another group as they all show a high-voltage capacity with the delivered extra capacity being inversely proportional to the current density, as mentioned before for Sn, with therefore an extra capacity which is quite less for the Pb-based films. Additionally, we experienced a total disappearance of the extra capacity displayed by Sn, Pb, and Bi thin films when Li/Sn, Li/Bi, Li/Pb coin cells were discharged vs. lithium using either EC-free or VC loaded EC–DMC 1 M $LiPF_6$ rather than EC–DMC 1 M $LiPF_6$ electrolytes, confirming again the importance of EC in governing the 1.5 V extra capacity.

One can rightly argue that similar surface morphologies would have been ideal for meaningful comparison, however this could not be achieved in spite of the great effort placed on adjusting/tuning electrolytic bath formulations, electrodeposits currents (pulse vs. continuous), electrodeposits temperatures and potentials. Although there are definitely inherent errors in our measurements due to these differences in morphology, the large changes in extra capacity that we measured, depending upon the metal element, were by far greater than those we could measure on Sn deposits of drastically different morphologies; this gave us confidence that our established trends between the reactivity of Sn, Pb, Si, Sb ad Bi are robust.

3.3. Sn/C composites

At this stage there remains a puzzling question dealing with the appearance of this phenomenon with carbon-free Sn electrodeposited thin films made of bare tin particles while it has never been reported for Sn/C composites. To gain further insight into this issue, composite electrodes using tin powders having a specific surface area of around 4 m^2 g^{-1}, containing 100 nm particles and 20% carbon super P as electronic additive were made. Fig. 9 shows the voltage discharge–charge profiles for this composite electrode (prepared by doctor blade method) vs. Li that was cycled at low current (10 mA cm^{-2}). A tiny extra electrochemical activity can be observed at high voltage and its slight dependence with varying the current amplitude suggests that is origin is as before nested in the EC electrolyte degradation.

Along that line, Sn/C composite electrodes made from Sn metal organic precursors should not show extra capacity at 1.5 V, as such electrodes do contain pristine Sn surface like all the particles intimately protected by carbon [28]. We reinvestigated the electrochemical reactivity of such composites and sure enough, regardless of the lowest discharge current we used (<C/100), we could never trigger the appearance of a 1.5 V plateau although the irreversibility is abnormally high, exceeding 150% of the initial discharge capacity. This clearly indicates that such extra capacity in these composites does not come from pristine surfaces but more from subtle properties of the carbon matrix (presence of heteroatom, remaining carboxyl groups) not yet identified. This conclusion was further supported by the observed constancy of the irreversible capacity for Sn/C composites regardless of whether we were using EC-free or EC–DMC electrolytes (Fig. 10). As we could not succeed in reducing the irreversible capacity of Sn/C composites via electrolyte formulation, we searched for alternative approaches. We found that this irreversible capacity could be reduced by a pre-treatment of the Sn/C composite electrode. This pre-treatment consists in bringing it for a few minutes in close contact with an electrolyte-wetted metallic lithium (e.g., capillary contact) so as to favour, prior to the cell assembly, most of the irreversible processes that are responsible for the initial capacity loss. These mainly include decomposition of the electrolyte with the formation of a protective film on the electrode surface and reaction of residual minor impurities, e.g., tin oxide. This way, we could reduce the initial irreversible capacity of a Sn/C electrode in a lithium cell (Fig. 11) using a (EC–DMC)-based electrolyte to a great extent (e.g., from 600 mAh g^{-1} for an untreated electrode to a value of the order of 30–40 mAh g^{-1} for a treated electrode). Further details of this treatment, which is beyond the scope of this paper, will be published in the forthcoming months.

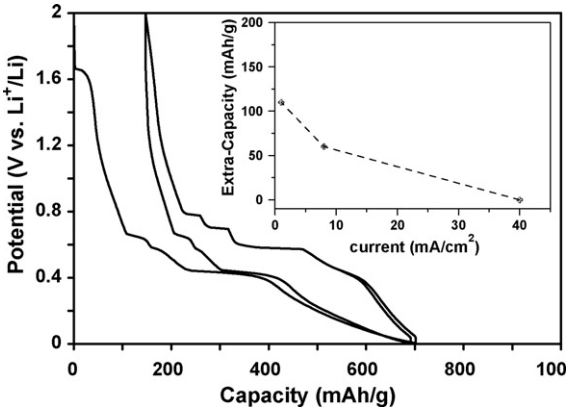

Fig. 9. Galvanostatic profile (40 mA g^{-1}) for Sn–20%Csp/Li cell with EC–DMC 1 M $LiPF_6$ electrolyte together with an inset of the "1.5 V plateau" capacity dependence with applied specific current.

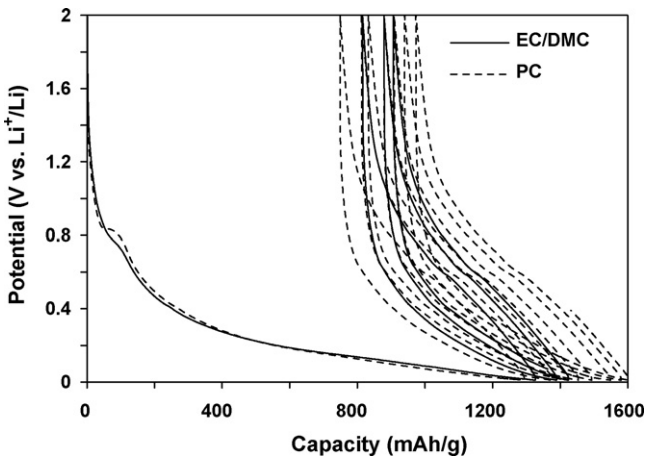

Fig. 10. Voltage vs. capacity for (Sn/C)/Li cells using Sn/C composites (made according to Ref. [13]) as the positive electrode. Regardless of the electrolyte used, the curves are alike suggesting that the large irreversible capacity observed in these composites has a different nature. The data was collected in a galvanostatic mode at C/9 of SnC using either PC $LiPF_6$ or EC–DMC $LiPF_6$ electrolytes.

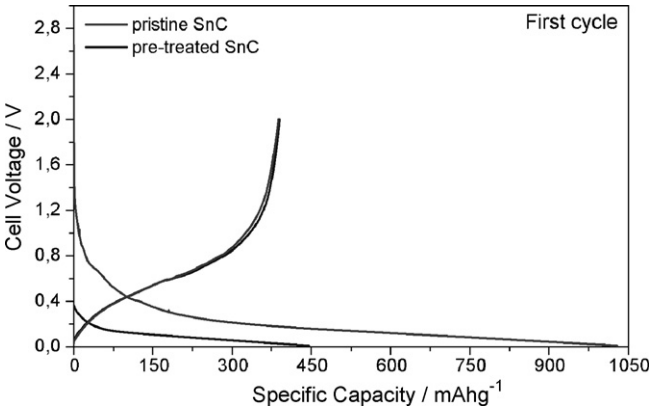

Fig. 11. Voltage vs. specific capacity profiles of the Sn/C electrode cycled galvanostatically in a lithium cell at a pristine state and after the pre-treatment described in the text. Electrolyte: EC–DMC $LiPF_6$. Charge–discharge current density: 100 mA cm^{-2} g^{-1}.

4. Discussion/conclusions

The anomalous high-voltage irreversible capacity observed during the reduction of tin by Li was previously assigned, via AFM measurements [17], to electrolyte decomposition catalyzed by pure tin surfaces. Our present study not only confirmed this assignment but also went one step further by providing direct evidence for an electrochemically driven decomposition of ethylene carbonate catalyzed by fresh Sn surfaces. This finding is the result of IR studies which show that the layer formed during reduction contains, besides Li_2CO_3, products such as lithium methyl carbonate, the presence of which can simply be explained from EC and DMC degradation schemes; but more importantly it shows our ability to get rid of this extra capacity by using EC-free electrolyte or VC loaded EC–DMC electrolytes. Therefore, since Sn catalyzes the decomposition of EC leading to the growth of a layer at its surface, one could expect (1) the film cyclability to decrease with increasing extra capacity (e.g., with increasing the layer thickness) and (2) the polarization resistance to increase due to the Li-ionic diffusion barrier created by the growing layer, as we experimentally observed. In the presence of EC-free electrolyte, there is indeed no extra capacity at 1.5 V, or formation of a passivating layer (as deduced by SEM) explaining why the cells were showing sustained reversibility with limited polarization. We showed that good cycling can be obtained by adding a reasonable amount of VC (<10%) to EC–DMC-based electrolyte. The magic of VC is that it decomposes at 2.5 V vs. Li^+/Li° on Sn surface (not shown here) leading to the formation of oligomers, which coat the electrode particles, and then prevent further copious electrolyte decomposition at lower potentials. When not enough VC is used, one can expect an imperfect particle coating, this was experimentally observed as 2% of VC was not sufficient to remove the 1.5 V extra capacity whereas 10% was. It is surprising that on carbon electrodes the EC–DMC degradation only occurs for potentials lower than 1 V while VC was shown to start decomposing at 1.25 V (as deduced by XPS measurements)[24] while, on Sn electrodes these potentials are 1.5 and 2.5 V, respectively. However, when dealing with catalytic-driven decomposition reactions (e.g., the supporting electrode being the catalyst), such a swing in the redox degradation potentials of various organic molecules is feasible and the literature is full of examples. Redox degradation potentials can be determined from thermodynamic calculations and in the case of EC, assuming the following degradation reaction [EC (liq) + 2Li = Li_2CO_3 (s) + C_2H_4 (g)] and not taking into account corrections from solvated species, we obtained a value of 2.25 V, which is quite higher than what we observed. This reminds us that the Li-ion technology relies on the use of electrolytes which operate beyond their thermodynamic stability range. This is the result of sluggish solvent degradation kinetics, and fortunately Nature has been very cooperative up to now. Tin electrodeposited electrodes, which favour electrolyte degradation at higher voltages, seem to be an exception.

We also demonstrated that such a metal-catalyzed EC decomposition was not specific to Sn but could also occur with Bi and to a lesser extent with Pb, via a survey of the electrochemical reduction of various metal electrodeposits vs. lithium. Similarly, In deposits were also found (data not reported for reasons of length) to trigger EC decomposition. In contrast, other metals capable of alloying with Li, such as Si or Sb, showed no catalytic activity towards EC decomposition. Thus, it remains important to understand the origin of different behaviour among the metals investigated. Most of these metals, in their oxidized state Bi^{3+}, Sn^{2+}, Sb^{3+}, or Pb^{2+}, have s_2 lone pairs, so one could be tempted to relate the presence of lone pairs to the metal catalytic activity; therefore the non-activity of Sb towards EC decomposition invalidates such a tentative correlation. Purely coincidentally or not, turning to the field of organic chemistry, metallic Sn and Bi are among the most used metal catalysts, while we are not aware of any organic synthesis schemes calling for the use of Si metal. So, although we do not fully understand the origin of this specific activity, it turns out, whether purely coincidentally or not, that our results are along the line of previous observations dealing with the electrochemical reduction of carbon dioxide on flat metallic substrates for which a greater activity was reported for sp (Sn, Pb, In) rather than 3d (Si) group metal substrates [29]. We are motivated to get further insight into the mechanism underlying the Sn catalytic process as it could simplify our understanding of metallic-based negative electrodes. Sn *in situ* Mössbauer on a Sn/Li electrochemical cell is presently being performed to get further insight into the mechanistic associated to the Sn catalytic-driven EC decomposition process.

Lastly, a legitimate question deals whether such a Sn, Bi and Pb, to a lesser extent, metal activity towards electrolyte decomposition is specific to EC or can be extended to other cyclic carbonates such as PC, for instance. To our total surprise, Sn/Li cells cycled in PC rather than EC-based electrolytes did not show a significant 1.5 V plateau, regardless of the low discharging current we have used (C/100). Besides the fact that PC is a stronger donor (i.e. more solvating than EC), another difference between such molecules is that PC is a larger molecule than EC due to the presence of the methyl group. Such a geometric difference could be essential for

catalytic reactions which at one stage must involve the adsorption of the molecules onto the catalyst. Owing to the geometric hindrance provided by the methyl group, the PC molecules might interact differently than the EC-ones with the tin electrodeposited surface electrode and therefore be less subject to degradation. We must therefore admit that this difference in reactivity between EC and PC molecules, which are very similar, is a problem. We presently know that ethylene carbonate (EC) can provide the ad hoc protective layer on graphite surface to avoid further reaction (continuous electrolyte reduction and self-discharge). However we do not know why the homologous propylene carbonate is unsuitable for this protective layer; just a reminder that chemistry has its secrets. The drastically different reactivity of EC and PC with respect to tin electrodeposited surfaces adds another one, which we hope further ongoing studies will clarify.

Acknowledgments

We thank A. Finke for his contribution with the fabrication of the films, M. Armand for fruitful discussions and the network of excellence ALISTORE for having nucleated this work.

References

[1] N.P. Yao, L.A. Heredy, R.C. Saunders, J. Electrochem. Soc. 118 (1971) 1039.
[2] S.-C. Lai, J. Electrochem. Soc. 123 (1976) 1196.
[3] W. Weppner, R.A. Huggins, J. Electrochem. Soc. 124 (1977) 1569.
[4] W. Weppner, R.A. Huggins, J. Solid State Chem. 22 (1977) 297.
[5] R.A. Huggins, Solid State Ionics 113–115 (1998) 57.
[6] I.A. Courtney, J.R. Dahn, J. Electrochem. Soc. 144 (1997) 2045.
[7] J.H. Ryu, J.W. Kim, Y.E. Sung, S.M. Oh, Electrochem. Solid-State Lett. 7 (2004) 306–309.
[8] A.M. Wilson, J.R. Dahn, J. Electrochem. Soc. (1995), 142. 326.
[9] A.M. Wilson, J.R. Dahn, J. Electrochem. Soc. 142 (1995) 326.
[10] W.R. Liu, M. Yang, H. Wu, S.M. Chiao, N. Wu, Electrochem. Solid-State Lett. 8 (2005) A100.
[11] N.S. Hochgatterer, M.R. Schweiger, S. Koller, P.R. Raimann, T. Wöhrle, C. Wurm, M. Winter, Electrochem. Solid-State Lett. 11 (5) (2008) A76–A80.
[12] B.A. Boukamp, G.C. Lesh, R.A. Huggings, J. Electrochem. Soc. 127 (1981) 725–728.
[13] G. Derrien, J. Hassoun, S. Panero, B. Scrosati, Adv. Mater. 19 (2007) 2336–2340.
[14] N. Tamura, R. Ohshita, M. Fujimoto, S. Fujitani, M. Kamino, I. Yonezu, J. Power Sources 107 (2002) 48.
[15] S.D. Beattie, T. Hatchard, A. Bonakdarpour, K.C. Hewitt, J.R. Dahn, J. Electrochem. Soc. 150 (6) (2003) A701–A705.
[16] M. Inaba, T. Uno, A. Tasaka, J. Power Sources 146 (2005) 473–477.
[17] L.Y. Beaulieu, S.D. Beattie, T.D. Hatchard, J.R. Dahn, J. Electrochem. Soc. 150 (4) (2003) A419–A424.
[18] A. Finke, P. Poizot, C. Guéry, J.-M. Tarascon, J. Electrochem. Soc. 152 (12) (2005) A2364–A2368.
[19] A. Finke, PhD Thesis, UPJV 2007.
[20] S.S. Abd El Rehim, A. Awad, A. El Sayed, J. Appl. Electrochem. 17 (1987) 156–164.
[21] Y. Nishimura, Y. Fukunaka, Electrochim. Acta 53 (2007) 111–116.
[22] D. Aurbach, M.L. Daroux, P.W. Faguy, E. Yeager, J. Electrochem. Soc. 134 (1987) 1611–1620.
[23] L. Gireaud, S. Grugeon, S. Laruelle, S. Pilard, J.-M. Tarascon, J. Electrochem. Soc. 152 (2005) A850–A857.
[24] R. Dedryvère, S. Laruelle, S. Grugeon, L. Gireaud, J.-M. Tarascon, D. Gonbeau, J. Electrochem. Soc. 152 (4) (2005) A689–A696.
[25] D. Aurbach, K. Gamolsky, B. Markovsky, Y. Gofer, M. Schmidt, U. Heider, Electrochim. Acta 47 (2002) 1423–1439.
[26] L. El Ouatani, R. Dedryvère, C. Siret, P. Biensan, S. Reynaud, P. Iratçabal, D. Gonbeau, J. Electrochem. Soc. 156 (2) (2009) A103–A113.
[27] O. Matsuaka, A. Hiwara, T. Omi, M. Toriida, T. Hayashi, C. Tanaka, Y. Saito, T. Ishida, H. Tan, S.S. Ono, S. Yamamoto, J. Power Sources 108 (2002) 128.
[28] J. Hassoun, S. Panero, P. Reale, B. Scrosati, Adv. Mater. 21 (2009) 1–4.
[29] M. Jitaru, D.A. Long, M. Toma, L. Oniciu, J. Appl. Electrochem. 27 (1997) 875–889.